19th Brazilian Congress of Thermal Sciences and Engineering
November 06th-10th, 2022, Bento Gonçalves - RS - Brazil

ENC-2022-0349
DETERMINATION OF THERMAL PROPERTIES AT HIGH TEMPERATURES BY THE APPLICATION OF AN OPTIMIZED INVERSE PROBLEM METHODOLOGY

Ernandes José Gonçalves do Nascimento
Arthur Mendonça de Azevedo
Elisan dos Santos Magalhães
Instituto Tecnológico de Aeronáutica – ITA, São José dos Campos – SP, Brasil
ernandesn549@gmail.com
arthurama@ita.br
elisan@ita.br

Abstract. *The evolution of engineering design techniques created a demand for determining material parameters under severe working conditions. However, the application of direct experimentation methods in measuring thermal properties usually does not provide accurate results for high-temperature appliances. The present work demonstrates the use of an inverse methodology numerical tool that makes possible the estimation of the thermal properties of a material at high-temperature values. The presented technique is an optimization method developed to eliminate the need for direct experimental measurements. The applied approach consists of a multivariable model developed to estimate the specific heat function's parameters. A laser beam welding problem (LBW) was simulated in three dimensions to exemplify the efficiency of the proposed methodology. The partial differential heat conduction equation was converted into an algebraic form by employing the Finite Volume Method (FVM). The enthalpy method was applied by means of the Heaviside step function to account for the phase change in the weld bead. The Time-Traveling Regularization (TTR) scheme was applied in the objective function to regularize the results. The welding laser beam was modeled as a 3D gaussian volumetric heat source. Temperature-dependent thermal properties were applied to the welded specimen material. A parallelized in-house CUDA-C (Compute Unified Device Architecture) language code was specifically developed to simulate the autogenous welding problem. The software computed the unsteady state simulation by running in a Graphical Processing Unit (GPU) instead of the standard Central Processing Unit (CPU) methodology. The Nvidia RTX3060 video card was used as simulating hardware device. Finally, a simulated welding experiment was performed to validate the proposed approach and estimate the real experimental errors. The proposed inverse problem tool demonstrated a very low specific heat average error. The enhanced methodology can reduce costs and increase accuracy compared to traditional advanced experimental apparatus applied in the direct measurement of thermal properties at high temperatures.*

Keywords: *Inverse problems, Numerical phase change, Finite Volume Method, GPU processing, CUDA-C language.*

1. INTRODUCTION

The direct measurement of material properties at high temperatures remains as a noticeable challenge in thermal engineering. The thermal isolation of unwanted phenomena such as convection or radiation is harder as the temperatures involved in the process rise. Simultaneously, the higher the temperatures of measurements, the more relevant are the loss quantities, which in turn results in less accuracy and reliability in the final value. Consequently, the cost of direct experimentation measurements at high temperatures is very high due to expensive laboratory apparatus, material losses, qualified labor, and the need for thermal equilibrium to be reached, which in some cases means long hours of waiting. Adding to the previously cited issues, many new materials are constantly arriving at the market and the thermal properties must be known for engineering design purposes. Hence, one may easily infer that there is a costly technological bottle neck slowing down the evolution from new materials development and a cheaper and more reliable engineering design, usually performed by extensive simulations.

Historically, the gaps in direct experimentation have been fulfilled by inverse problems methodologies. This field have been widely researched during the twentieth century and has its main roots in the development of optimization techniques. For instance, in Sparrow *et al.* (Sparrow, Haji-Sheikh, & Lundgren, 1964) presented in 1964 a general

theory for determining the temperature and heat flux at the surface of a solid when temperature at an interior location is a prescribed function time. This theory was able to suit an initial temperature distribution that varies arbitrarily with the position throughout the solid. The method had its accuracy demonstrated by a numerical example, which became popular among researchers of the field for providing smooth and non-oscillatory results.

James Beck was noticeably one of the first researchers to remarkably apply inverse techniques to the solution of engineering thermal problems. The author presented a family of methods (Beck, Surface heat flux determination using an integral method, 1968) for calculating the surface heat flux from the transient temperature history measured at an interior position in a heat-conducting solid with constant thermal properties. The methods involved the numerical inversion of a convolution integral with the employment of a least-squares procedure. The proposed approach had evolved from the methods previously given by Stolz (Stolz, 1960). However, significant improvement was reached by the implementation of much smaller time steps. Rizzo (Rizzo & Shippy, 1970) developed a numerical treatment of classical boundary value problems for generalized shaped plane heat conducting solids obeying Fourier's law. An exact integral formula determined on the boundary of an arbitrary body was obtained from a fundamental singular solution to the governing differential equation. The method was performed with a numerical transform inversion with all operations ideally suited for modern digital computation. Imber and Khan (Imber & Khan, 1972) described an analytical method developed for the inverse heat conduction problem when the temperatures are known at two positions. The method could be used to determine boundary conditions at a face of a finite slab or a hollow sphere, with high accuracy. The resultant temperature extrapolation was also feasible for multilayered mediums. The analytical solution was verified by numerical examples to enhance reliability. Two years later, Imber (Imber, Temperature extrapolation mechanism for two-dimensional heat flow, 1974) proposed a temperature extrapolation mechanism for two-dimensional heat flow. This study was a groundbreaker due to being one of the first solutions to inverse problems applicable to two-dimensional conduction systems or geometries of arbitrary shape. The technique made use of a temporal power series approximation of the input or thermocouple data to facilitate the computation of the desired temperatures, since computational power was very limited at the time. Alifanov and Mikhailov (Alifanov & Mikhailov, 1978) developed the solution of the nonlinear inverse thermal conductivity problem by an iteration method. The authors presented a regular iteration algorithm based on the method of conjugate gradients constructed for the case of a nonlinear generalized thermal conductivity equation for determining an unsteady thermal flux. Following the evolution of inverse problem methodology, Beck published then a series of criteria (Beck, 1979) for comparison of methods solution for inverse heat conduction problems. The content included accuracy when using exact data, insensitivity to measurement errors and stability for small time steps. The criteria were applied to the method previously developed and published in 1968. Subsequently, Weber (Weber, 1981) developed a special solution procedure for the one-dimensional case which replaces the heat conduction equation with an approximating hyperbolic equation. Sample calculations performed by the author confirmed that the published approach produced consistent and reliable results. Beck *et. al* (Beck, Litkouhi, & St. Clair Jr., 1982) developed an efficient sequential solution of the nonlinear inverse heat conduction problem. The general heat conduction model was used to treat various one-dimensional geometries (plates, cylinders, and spheres), energy sources and fin effects. The approach was first demonstrated with the use of Finite Differences Method (FDM). However, the concepts were also applicable to the Finite Volume Method (FVM).

Fast forwarding to the twentieth first century, the great evolution in computational hardware and CFD had made possible a deeper and more efficient use of the inverse problems techniques. For instance, Lee and Yan (Lee & Yan, 2017) proposed a solution to one-dimensional inverse heat conduction problems (IHCP) that require a relatively long time. A hybrid technique was applied to analyze the laser surface heating and spray cooling on a hot surface. The results contained an estimation of the unknown temperature function in half-range expansions form. The coefficients of half-range expansions could be determined by using the least-squares method in conjunction with the estimated temperature and experimental data. Han *et al.* (Han, Chen, & Lu, 2019) applied a IHCP approach in the estimation of a time-dependent convective boundary condition in a horizontal pipe with thermal stratification. The optimization was accomplished by the conjugate gradient method (CGM) and the method was validated by seven experiments under different conditions. The research concluded that the increase of volume flow rate of cold water resulted in the increase of the convective heat transfer coefficient, and the temperature distribution of the pipe wall resulted in different characteristics. Kolesnik and Bulychev (Kolesnik & Bulychev, 2020) proposed an analytical method for solving the inverse problem of identification of components of the thermal conductivity tensor in anisotropic materials based on the earlier analytical solution of heat conduction in anisotropic half-space when heated with a thermal flow. The method was based on expansion of the residual functional into Taylor series and determination of incremental vectors of the target coefficients. The solution demonstrated fine iteration convergence even if the initial approximation of the coefficients vector differs from the target one by several time, or even if there is inaccuracy in the experimental data. Hosejowska and Piasecka (Hożejowska & Piasecka, 2020) developed a numerical solution for an axisymmetric IHCP by the trefftz method. The paper was focused on determining the boiling heat transfer coefficient at the HFE-649 fluid-heater contact during flow along an annular minigap. The mathematical model assumed that the fluid flow was laminar, and the heat transfer was a steady state process. The Trefftz method was considered convenient because it yields solutions that exactly satisfies the governing equation. Hun *et al.* (Noh, Kwak, Kim, Cha, & Yook, 2018) applied a three-dimensional inverse heat conduction modeling to predict heat flux in a hollow cylindrical tube with irregular cross

sections. An introduction to an experimental method for estimating heat flux by measuring the surface temperatures of real gun barrels was also made. The average values of heat flux revealed that the heat flux tended to decrease with respect to position toward the exit ends of the barrels (point 5).

The traditional thermal inverse problems methodology lacks faster solutions due to being computationally intensive. Most methods developed until now are either analytical or numerical with not significant improvements in parallelization and computational time. As the IHCP approaches advance, higher computational power is required to solve the higher complexity of thermal problems, leaving plenty of space to be filled with the evolution of numerical methods. Hence, in the current work a demonstration of a parallelized IHCP run in GPU was performed. A Laser Beam Welding (LBW) process with an automated moving heat source was simulated to demonstrate the methods effectiveness. The simulations were run in an inhouse code developed using CUDA-C language, by Nvidia™, and the SOR (Successive over-relaxation) parallelized solver. The heat conduction partial differential equation (PDE) with an added phase-change term was transformed into an algebraic equation and discretized in a three-dimensional domain by the application of the Finite Volume Method (FVM). Temperature dependent thermal properties were applied to the welded specimen material. The enthalpy method was applied to account for phase changes in the material by numerically calculating the drop in temperature due to the latent heat of fusion. The thermal modeling accounted for radiation and convection losses in the specimen. The inverse analysis was performed by successive simulations with the application of a Future Time Regularization (FTR) implemented in the objective function to regularize the results. The final estimated welding parameter was compared to a simulated welding experiment data. The research outcomes had suggested that the applied methodology has enough potential for replacing traditional CPU processing techniques. The parallelization approach employed had demonstrated the capability of significative costs reduction by minimizing time expenditure, computational costs and required laboratory apparatus.

2. BASIC CONCEPTS AND METHODOLOGY

2.1 Inverse Heat Conduction Problem (IHCP)

The current experimental methods for direct measurement of material parameters in a high temperature process usually do not provide good quality values. Hence, it is possible to estimate the parameters numerically by sequentially simulating the process and comparing the results with the experimental temperature field. In previous work, Magalhães (Magalhães, 2021) presented an inverse problem heat conduction technique for the estimation of non-linear thermal properties of materials submitted to high temperature gradients. The work developed here is an example application of the original method. For the sake of concision, the applied methodology will be resumed to the most important calculations. The IHCP approach is a multivariable estimation technique developed to determine the function's parameters. In this work, the specific heat is estimated through the inverse tool for a LBW process. In this case, the specific heat was treated as an exponential function. As part of the inverse methodology, to regularize the results, the Future Time Regularization (FTR) scheme is applied. This calculation may be mathematically expressed as:

$$F = \sum_{p=0}^{r} \sum_{s=0}^{n_s} (T_{P,p}^{s} - T_{Se,p}^{s})^2 \tag{1}$$

where T is the temperature, r is the number of future time steps, n_s is the number of temperature sensors, P is the numerical temperature sensor, and Se is the experimental sensors.

2.2 Mathematical Modeling

The applied heat conduction model is composed of the non-linear three-dimensional heat diffusion differential equation (Versteg & Malalasekera, 2007), with phase change modeling performed through an enthalpy function. The mathematical modeling may be represented as:

$$\frac{\partial}{\partial x}\left(\lambda \frac{\partial T}{\partial x}\right) + \frac{\partial}{\partial y}\left(\lambda \frac{\partial T}{\partial y}\right) + \frac{\partial}{\partial z}\left(\lambda \frac{\partial T}{\partial z}\right) + \dot{g} = \frac{\partial H}{\partial t} \tag{2}$$

where x, y and z are the cartesian coordinates, λ is the non-linear thermal conductivity, T is the numerical temperature, $\dot{g}$ is the volumetric heat source, t is the time and H is the total enthalpy density, which may be written as (Crank, 1984),

$$H = \rho \int_{0}^{T} c_p(\phi)\, d\phi + \rho f(T) L \tag{3}$$

where ρ is the density, c_p is the specific heat at constant pressure, ϕ is the integration variable, L is the latent heat of fusion and f is the Heaviside step function, which is expressed as:

$$f = \begin{cases} 1 \text{ if } T < T_m \\ 0 \text{ if } T > T_m \end{cases} \tag{4}$$

where T_m is the temperature of fusion.

The specimen was subjected to forced and natural convection and radiation. The first of them was caused by the shielding gas flow, which moved with the LBW heat source. This work considered the forced convection in the modeling of the shielding gas influence, which is assumed to be similar to a Single Round Nozzle (Martin, 1977). Additionally, the radiation of the specimen was also considered. Therefore, this boundary condition can be written as:

$$\frac{\partial T}{\partial \eta} = h(T)\left(T - T_\infty\right) + \sigma\phi_{rad}(T)\left(T^4 - T_\infty^4\right) \tag{5}$$

where η is the direction normal to the surface, $h(T)$ is the convection as a function of temperature, σ is the Stefan Boltzmann constant and ϕ_{rad} the material's emissivity.

The LBW heat source modeling is shaped as a gaussian conical volumetric heat distribution, as exposed in Fig. Figure **1**. The mathematical description of the moving heat source is given as (Magalhães, 2021):

$$\dot{g} = \frac{Q_W}{0.460251 h_p R^2} e^{-\frac{4.5(z-ut)^2}{R^2}} e^{-\frac{4.5\left(y-L_y/2\right)^2}{R^2}} \left(1 - \frac{x^{1/2}}{h_p^{1/2}}\right) \tag{6}$$

where Q_w is the LBW power, h_p is the height of penetration, R is the welding radius and u is the welding head velocity.

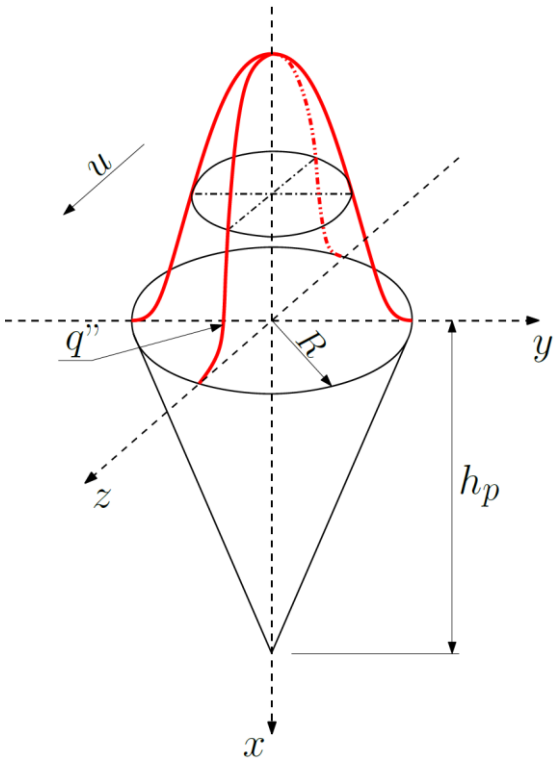

Figure 1. Mobile volumetric heat source modeling.

2.3 Simulation Domain, Parameters and Material Properties

The domain of solution of Eq. ($\frac{\partial}{\partial x}\left(\lambda\frac{\partial T}{\partial x}\right)+\frac{\partial}{\partial y}\left(\lambda\frac{\partial T}{\partial y}\right)+\frac{\partial}{\partial z}\left(\lambda\frac{\partial T}{\partial z}\right)+\dot{g}=\frac{\partial H}{\partial t}$ (2 is represented in Figure 2. The measurements L_x, L_y and L_z are the domain dimensions in the x, y and z directions, Q_w is the heat input from the welding head source, Q_{rad} is the heat loss by radiation and Q_{con} is the heat loss by convection.

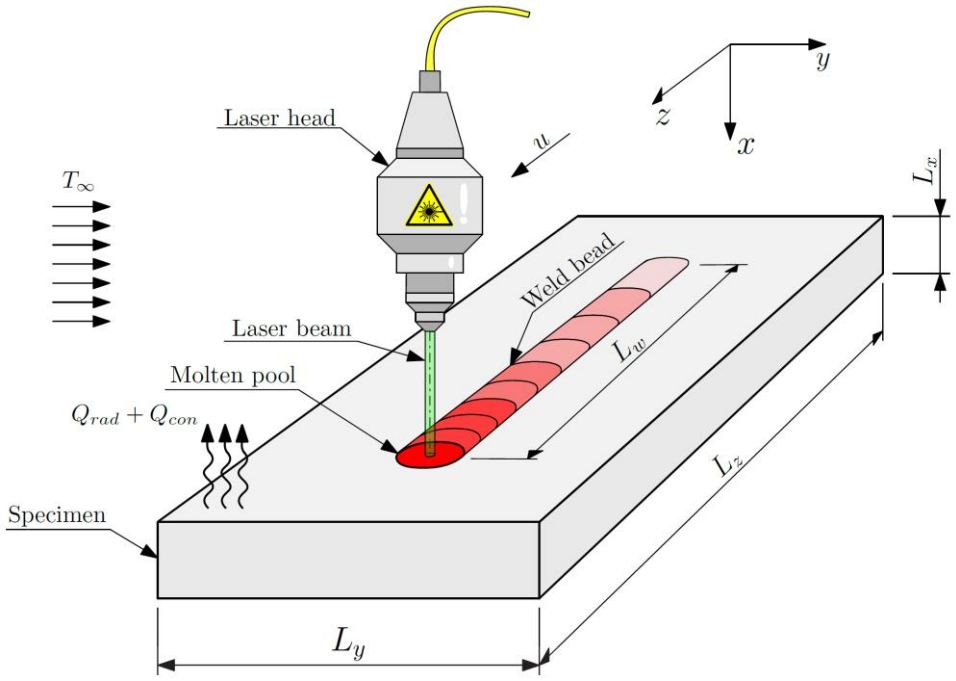

Figure 2. Simulated Laser Beam Welding (LBW) experiment.

The welded material was a SAE1020 steel sample. The simulated physical apparatus was composed of a fiber laser power source of 3000 W. The values for the weld penetration and bead radius are h_p = 1.65 mm and R = 0.5 mm, respectively. The applied melting temperature was 1450.0 ºC. Table 1 presents the additional simulation parameters and SAE 1020 steel thermal properties.

Table 1. Simulation parameters and SAE 1020 steel thermal properties.

Parameter	**Values**
L_x, L_y, L_z and L_w [mm]	9.5, 20.0, 40.0 and 30.0
u [mm/min]	3000.0
Time step [s]	0.01
Experimental time [s]	2.0
Welding radius, R [mm]	0.5
Height of penetration, h_p [mm]	1.65
Laser power, Q_w [W]	1000.0
Thermal properties (SAE 1020)	**Values / Equations**
λ [W/m.K]	$\lambda(T)=2.5\times10^{-5}T^2+57,2$
c_p [J/kg.K]	$\rho c_p(T)=2.55\times10^6 e^{1.51\times10^{-3}T}$
ε	0.8
ρ [kg/m³] and L [kJ/kg]	7,832.0 and 250.0
Melting Temperature, T_m	1450.0

The temperatures were acquired in the direct model with a reading rate of 0.01 s. Nine thermocouples were placed in the top surface of the specimen. The process was set to achieve the highest possible sensitivity to result in valuable data for the thermal conductivity estimation. The y and z axes coordinates for the positions of the sensors are described in Table 2.

Table 2. Positions of sensors in y and z axes.

Sensor	A01	A02	A03	A04	A05	A06	A07	A08	A09
y [mm]	0.10	0.11	0.12	0.13	0.14	0.15	0.16	0.17	0.18
z [mm]	0.20	0.20	0.20	0.20	0.20	0.20	0.20	0.20	0.20

A grid size independence study has demonstrated that the simulation outputs became independent of mesh refinement at 150,000 total nodes. Therefore, the problem was simulated with a structured mesh size of 192,000 total nodes. A time-step size independence analysis with fixed values was also addressed. Results became independent of temporal grid refinement for values equal or smaller than $3{,}7 \times 10^{-2}$ s. As a result, a time-step size of 10^{-2} s was applied.

The parameter estimated in the inverse problem solution presented in this work is the thermal conductivity of a metal submitted to a generic laser welding process.

$$\lambda(T) = X_1 T^2 + X_2 \tag{7}$$

The estimated parameters for the search domain region had their conditions limited to the range: $1.0 \times 10^{-6} \leq X_1 \leq 1.0 \times 10^{-4}$ and $32 \leq X_2 \leq 83$. The target values were based on data published by Magalhães (Magalhães, 2021) and aimed at $X_1 = 2.5 \times 10^{-5}$ and $X_2 = 57.2$.

3. RESULTS AND DISCUSSION

In previous work, Magalhães (Magalhães, 2021) proposed that the sensitive coefficients are a function that variates with time. Therefore, the sensitivity of the estimative increases when more future time information is added to the IHCP approach. This information was replicated in the estimation of the thermal conductivity parameter.

In the first analysis, the direct model was applied to obtain the simulated temperature field. Secondly, the inverse methodology was applied to determine the parameters X_1 and X_2. For the case reported here, no random normalized error was added to test the stability of the method. The estimated values for different numbers of future time steps are presented in Table 3. The estimation results were in better agreement for $r \geq 140$. For $r = 20$ there was not enough sensitivity to reduce the $X_{1,\text{Error}}$. Nonetheless, for $r \geq 40$, the estimative of variable X_1 was performed with at least 2.070% accuracy (case with $r = 100$).

The best estimation was performed in the $r = 160$ case. As expected, a better agreement may be achieved when more future data is added into the estimation. More details may be inferred from the objective function: although the F value for $r = 20$ is relatively low, it does not represent a valuable try since this case does not results in enough sensitivity to perform the welding simulation.

The inverse methodology developed here may reach a local minimum error. For the $r = 40$, the estimation achieved satisfactory results. However, $r = 80$ made the method result in a local minimum again. For values of r higher than 140, a good estimation was then consistently found. When the sensitivity increases, the objective function becomes smother, leading to the expected estimation values.

Table 3. Estimated values for different values of r.

Variable	Goal	$r = 20$	$r = 40$	$r = 60$	$r = 80$	$r = 100$
X_1	2.5×10^{-5}	2.0916×10^{-5}	2.4977×10^{-5}	2.4970×10^{-5}	2.4977×10^{-5}	2.4493×10^{-5}
X_2	57.2	57.5000	57.2510	57.2021	57.2012	57.5498
F_{min}	0.000	0.54	3.145×10^{-2}	6.102×10^{-2}	6.053×10^{-2}	4.615×10^{-1}
$X_{1,\text{Error}}$	0.000 %	19.53%	0.092%	0.120%	0.092%	2.070%
$X_{2,\text{Error}}$	0.000 %	-0.521%	-0.089%	-0.004%	-0.002%	-0.608%

Variable	$r = 120$	$r = 140$	$r = 160$	$r = 180$	$r = 200$
X_1	2.4493×10^{-5}	2.4970×10^{-5}	2.4980×10^{-5}	2.4977×10^{-5}	2.4977×10^{-5}
X_2	57.5498	57.2012	57.2007	57.2012	57.2012
F_{min}	4.861×10^{-1}	5.552×10^{-2}	5.440×10^{-2}	5.583×10^{-2}	4.991×10^{-2}
$X_{1,\text{Error}}$	2.070%	0.120%	0.080%	0.092%	0.092%
$X_{2,\text{Error}}$	-0.608%	-0.002%	-0.001%	-0.002%	-0.002%

The local minimums present in the calculated errors ($X_{1,\,Error}$ and $X_{2,\,Error}$) as a function of the future time data (r) are illustrated in Figure 3. The lowest achieved errors were obtained for $r = 160$.

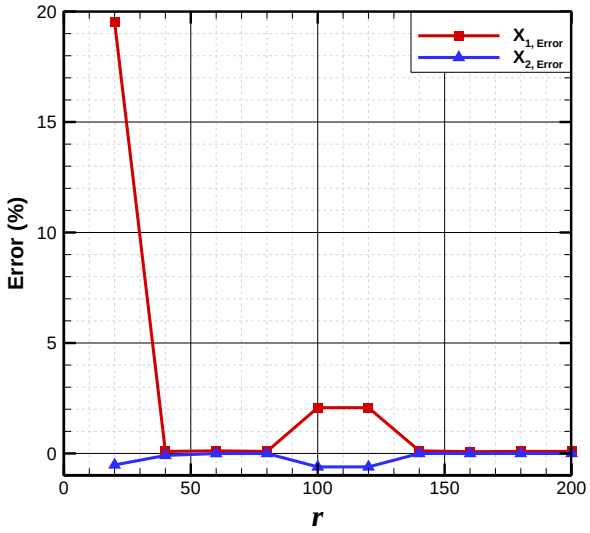

Figure 3. Local minimums of $X_{1,\,Error}$ and $X_{2,\,Error}$.

Figure 4 presents the contour plot for r = 20, which resulted in X_1 parameter not presenting a precise estimation. As it may be observed, the aimed parameter results in a local minimum outside the goal region (blue colour). This problem may happen when there is not enough sensitivity to perform the inverse investigation.

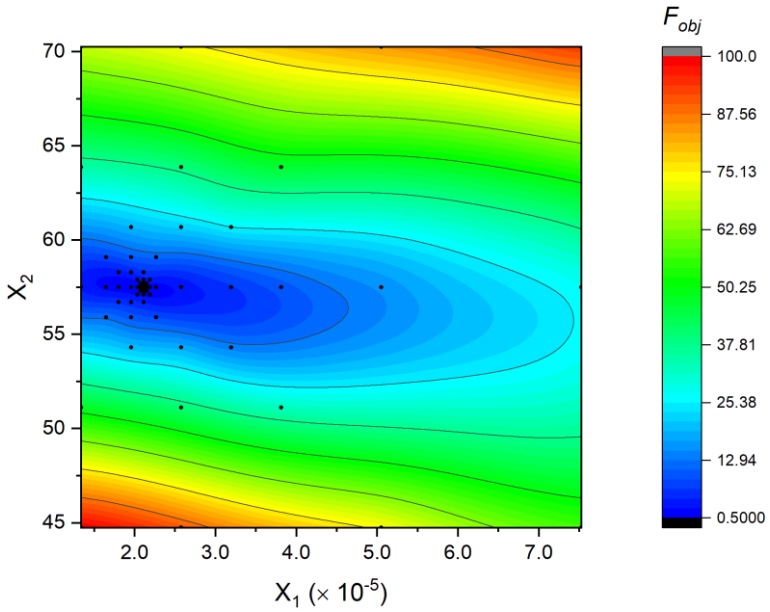

Figure 4. Objective function for r = 20 (normalized objective function scale).

The future information has the power to enhance the methods parametric guessing capability. Hence, one will certainly find better results by adding more detailing about future steps. To illustrate this, Figure 5 presents the objective function plot for four different future time values: (a) r = 40, (b) r = 80, (c) r = 120, and (d) r = 160. When r = 40, a similarity occurs in the objective function values. However, the difference is not big enough to achieve a precise estimation. By increasing r values once more, the objective function becomes smoother and thus the performed estimation better agrees with the goal.

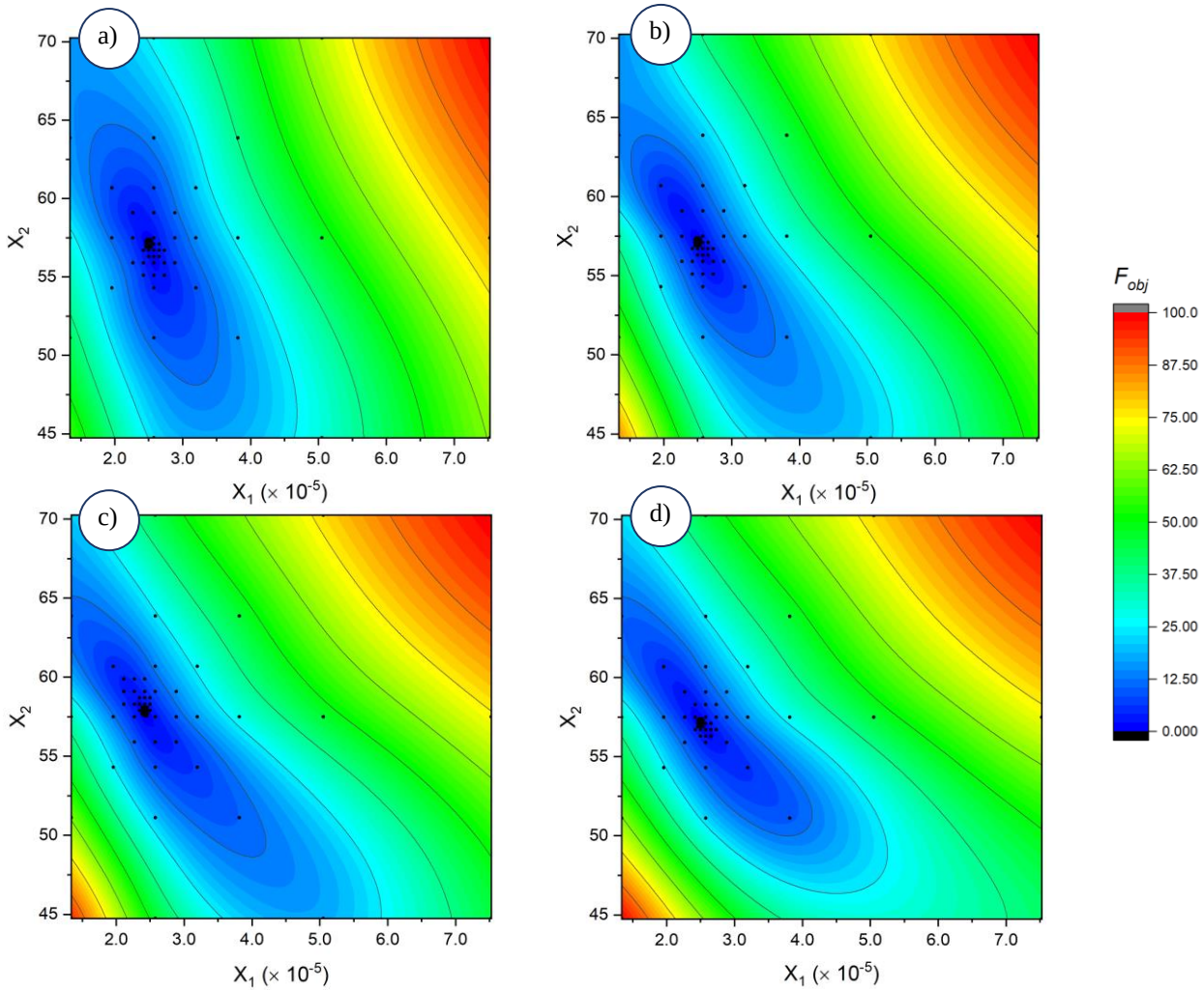

Figure 5. Objective function for future time values of (a) r = 40, (b) r = 80, (c) r = 120, and (d) r = 160.

As a final step, Figure 6 represents the LBW three-dimensional simulation of the case studied, at the instant t = 0.2 s. Figure 6a shows the temperature field on the north workpiece surface, where the heat source is applied. Furthermore, Figure 6b represents the longitudinal and transversal sections of the sample, making it possible to visualize the temperature distribution in the direction of the welding penetration height. These representations show that the proposed computational model, in addition to predicting the nonlinear thermal properties, allows the determination of the Heat Affected Zone (HAZ) temperature field. By applying this numerical methodology, the microstructural changes in the HAZ can be predicted. These, in turn, directly affect the material mechanical properties, such as ultimate tensile strength, hardness and toughness.

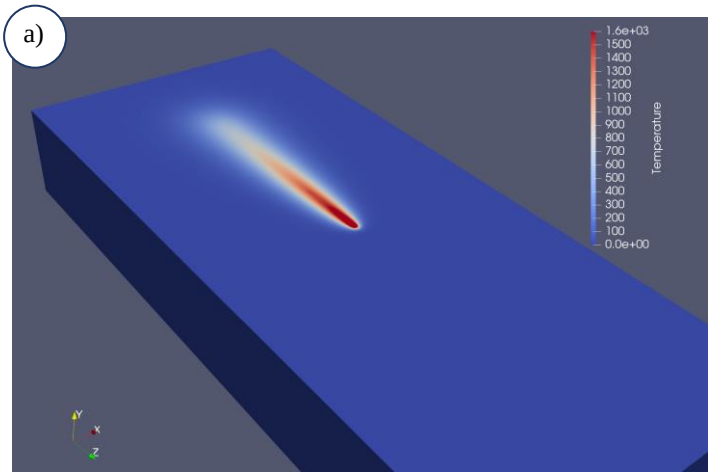

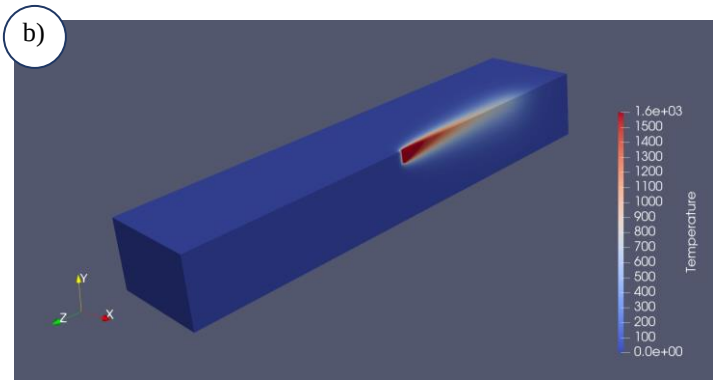

Figure 6. LBW simulation, where the temperature fields are shown (a) on the north surface and (b) in the direction of the welding penetration height.

4. CONCLUSION

This work presented an application of optimized inverse problem heat conduction methodology. The approach has proven to estimate thermal properties at high temperatures with reasonable accuracy. The exposed results have visually shown the effectiveness of the proposed optimization method by significantly reducing the original number of guesses present in the search area. The exposed method has given insight that it may be applied for more than two variables estimation or even more than one thermal property simultaneously.

5. REFERENCES

Alifanov, O. M., & Mikhailov, V. V. (1978). Solution of the nonlinear inverse thermal conductivity problem by the iteration method. *Journal of Engineering Physics*, 1501 - 1506.

Beck, J. V. (1968). Surface heat flux determination using an integral method. *Nuclear and Engineering Design*, 170 - 178.

Beck, J. V. (1979). Criteria for comparison of methods of solution of the inverse heat conduction problem. *Nuclear Engineering and Design*, 11 - 22.

Beck, J. V., Litkouhi, B., & St. Clair Jr., C. R. (1982). Efficient sequential solution of the nonlinear inverse heat conduction problem. *Numerical Heat Transfer*, 275 - 286.

Han, W. W., Chen, H. B., & Lu, T. (2019). Estimation of the time-dependent convective boundary condition in a horizontal pipe with thermal stratification based on inverse heat conduction problem. International Journal of Heat and Mass Transfer, 723 - 730.

Hożejowska , S., & Piasecka, M. (2020). Numerical Solution of Axisymmetric Inverse Heat Conduction Problem by the Trefftz Method. Energies, 1 - 14.

Imber, M. (1974). Temperature extrapolation mechanism for two-dimensional heat flow. AIAA Journal, 1089 - 1093.

Imber, M., & Khan, J. (1972). Prediction of transient temperature distributions with embedded thermocouples. AIAA Journal, 784 - 789.

Kolesnik, S. A., & Bulychev, N. A. (2020). Numerical analytic method for solving the inverse coefficient problem of heat conduction in anisotropic half space. *Journal of Physics: Conference Series*, 1 - 7.

Lee, S.-Y., & Yan, Q.-Z. (2017). Inverse analysis of heat conduction problems with relatively long heat treatment. *International Journal of Heat and Mass Transfer*, 401 - 410.

Magalhães, E. d. (2021). A quadrilateral optimization method for non-linear thermal properties determination in materials at high temperatures. *International Journal of Heat and Mass Transfer*, 1 - 10.

Noh, J.-H., Kwak, D.-B., Kim, K.-B., Cha, K.-U., & Yook, S.-J. (2018). Inverse heat conduction modeling to predict heat flux in a hollow cylindrical tube having irregular cross-sections. *Applied Thermal Engineering*, 1310 - 1321.

Rizzo, F. J., & Shippy, D. J. (1970). A Method of Solution for Certain Problems of Transient Heat Conduction. *AIAA Journal*, 2004 - 2009.

Sparrow, E. M., Haji-Sheikh, A., & Lundgren, T. S. (1964). The inverse problem in transient heat conduction. *Journal of Applied Mechanics*, 369 - 375.

Stolz, J. (1960). Numerical solutions to an inverse problem of heat conduction for simple shapes. *Journal of Heat Transfer*, 20 - 25.

Versteg, H. K., & Malalasekera, W. (2007). *An Introduction to Computational Fluid Dynamics.* Harlow, England: Pearson Education Limited.

Weber, C. F. (1981). Analysis and solution of the ill-posed inverse heat conduction problem. *International Journal of Heat and Mass Transfer*, 1783 - 1792.

6. ACKNOWLEDGMENTS

The authors would like to thank PETROBRAS, CAPES and CNPq, Brazil, for their invaluable financial support.

7. RESPONSIBILITY NOTICE

The author(s) is (are) the only responsible for the printed material included in this paper.